Journal of Inflammation Research Dovepress

Open Access Full Text Article ORIGINAL RESEARCH

Macrophage Infiltration Correlated with IFI16, EGR1 and MX1 Expression in Renal Tubular Epithelial Cells Within Lupus Nephritis-Associated Tubulointerstitial Injury via Bioinformatics Analysis

Ming Tian[1,2,*], Min Tang[1,2,*], Caiming Chen[1–3,*], Yufang Lin[1,2], Hong Chen[4], Yanfang Xu[1–3]

[1]Department of Nephrology, Blood Purification Research Center, the First Affiliated Hospital, Fujian Medical University, Fuzhou, People's Republic of China; [2]Fujian Clinical Research Center for Metabolic Chronic Kidney Disease, the First Affiliated Hospital, Fujian Medical University, Fuzhou, People's Republic of China; [3]Department of Nephrology, National Regional Medical Center, Binhai Campus of the First Affiliated Hospital, Fujian Medical University, Fuzhou, 350212, People's Republic of China; [4]Department of Pathology, the First Affiliated Hospital, Fujian Medical University, Fuzhou, People's Republic of China

*These authors contributed equally to this work

Correspondence: Hong Chen; Yanfang Xu, Email fychenhong@126.com; xuyanfang99@hotmail.com

Objective: A comprehensive bioinformatics analysis was conducted to investigate potential new diagnostic biomarkers and immune infiltration characteristics associated with tubulointerstitial injury in lupus nephritis (LN), and to examine possible correlations between key genes and infiltrating immune cells.

Methods: The GSE32591, GSE113342, and GSE200306 datasets were downloaded from the Gene Expression Omnibus database and differentially expressed genes (DEGs) were identified in the pooled dataset. Support vector machine-recursive feature elimination analysis and the least absolute shrinkage and selection operator regression model were used to screen for possible markers, and the compositional patterns of the 22 types of immune cell fractions in LN were determined using CIBERSORT. Finally, Western blotting, quantitative real-time polymerase chain reaction, and multiple immunofluorescence methods were used to confirm the significance of these feature genes in MRL/lpr mice and patients with LN.

Results: Seventeen DEGs were identified, of which 11 were considerably upregulated and six were markedly downregulated. Kyoto Encyclopedia of Genes and Genomes pathway analysis revealed significant enrichment in pertussis, complement and coagulation cascades, systemic lupus erythematosus, and other pathways. Based on the machine learning results, we identified *IFI16, EGR1* and *MX1* were key diagnostic genes for tubulointerstitial injury associated with LN. Immune cell infiltration analysis revealed that *IFI16, EGR1* and *MX1* were associated with M1 macrophages. Finally, the association between *IFI16, EGR1, MX1* and macrophages in MRL/lpr mice and patients with LN were verified.

Conclusion: This study suggests that *IFI16, EGR1* and *MX1* which are highly expressed in renal tubular epithelial cells in LN and are associated with macrophage infiltration, may be a novel diagnostic and therapeutic target.

Keywords: lupus nephritis, immune infiltration, tubulointerstitial injury, IFI16, EGR1, MX1

Introduction

Systemic lupus erythematosus (SLE) is a chronic autoimmune disease that affects several organs and tissues. Lupus nephritis (LN) is a serious complication of SLE. Approximately 70% of patients with SLE have clinical manifestations of renal damage, whereas 100% of patients have renal involvement on renal histopathology, immunofluorescence and electron microscopy.[1] LN is often characterized by hematuria, proteinuria, or decreased renal function. Renal impairment

Received: 22 August 2024
Accepted: 3 December 2024
Published: 24 December 2024

may be caused by glomerular, tubulointerstitial or vascular lesions.[2] LN, with a 10–20% risk of developing end-stage kidney disease within 10 years of diagnosis, is a major risk factor for death in patients with SLE.[3] Therefore, effective prevention and treatment of LN are urgently need.

The current pathological classification of LN by the International Society of Nephrology/Renal Pathology Society (ISN/RPS) is based entirely on glomerular lesions.[4] Whereas only 50–70% of patients treated according to the guidelines for the management of lupus nephritis achieve remission.[5] This also indicates that glomerular-centered classification criteria and treatment strategies do not well reflect the pathogenesis of the disease, and it is difficult to guide clinical precision treatment. It may exclude some other potentially important histopathological features that have a significant impact on the treatment and prognosis of LN.

There are two pathogenic mechanisms of LN: One involves glomerular and systemic autoimmunity, and the other involves tubulointerstitial and in-situ local adaptive immunity.[6] However, glomerular and tubulointerstitial lesions do not always coexist in patients with LN. Renal tubulointerstitial lesions can manifest as tubular epithelial cell injury, interstitial fibrosis, inflammatory cell infiltration, or other pathological changes. These are independent pathogenic factors for the onset of LN and have a direct impact on the poor prognosis of patients.[7,8] Although the degree of tubulointerstitial inflammation is more important in terms of prognosis than glomerulonephritic activity, the pathogenesis of tubulointerstitial injury in lupus nephritis is unknown and therefore there is no specific treatment regime.[5] Tubulointerstitial injury is believed to begin in the inflammatory process, and persistent interstitial inflammation has been shown to cause irreversible fibrosis and tubular atrophy. It is associated with progressive impairment of renal function.[9] In recent years, tubulointerstitial immune cell infiltration has attracted more and more attention. This is because tubulointerstitial inflammation is associated with in situ local adaptive immune cell networks. The aggregation of inflammatory cells in the interstitium can enhance antigen presentation and autoantibody production and aggravate tissue damage.[10] Immune cell infiltration determines the microenvironment of diseases, which in turn affects the immune response, and is the key to the pathogenesis and treatment of immune-related diseases. For example, lupus tubulointerstitial inflammation is associated with infiltrating B cells, plasma cells, T follicular helper cells (Tfh), plasmacytoid DCs (pDCs), and myeloid DCs (mDCs). These cell subsets are typically organized into lymphoid structures in the tubulointerstitium. This phenomenon is associated with local antigen-driven B-cell clonal selection, suggesting that adaptive immunity in the tubulointerstitium may play a role in driving renal outcomes,[11] but these processes are not fully understood. There are very limited studies systematically evaluating the characteristics of immune cell infiltration in the tubulointerstitium of LN. In addition to immune cell infiltration, renal tubular epithelial cells, as renal resident cells, can actively regulate tubulointerstitial immune cell responses through the production of soluble factors (such as pro-inflammatory cytokines and chemokines) and the expression of cell surface costimulatory and co-inhibitory molecules.[12] However, the relationship between immune infiltration and renal tubular epithelial cells is also poorly understood.

Therefore, in the present study, we used bioinformatics methods to obtain microarray data of renal tubular tissue of LN patients and healthy individuals from the GEO database. We performed differential expression analysis and enrichment analysis, etc.; at the same time, machine learning algorithms were used to screen biomarkers related to LN. Subsequently, immune infiltration analysis and correlation analysis were performed. Finally, quantitative reverse transcription-pcr (RT-qPCR), Western-blot and confocal immunofluorescence were used to verify the expression of these genes in renal tubulointerstitium of lupus mice and LN patients. The primary objective of these analyses is to provide new insights into the prevention and treatment of LN.

Materials and Methods

Microarray Data

Microarray data were searched in the Gene Expression Omnibus (GEO) database (http://www.ncbi.nlm.nih.gov/geo) using "systemic lupus erythematosus" and "lupus nephritis" as the keywords. The inclusion criteria were as follows: mRNA expression profile dataset from humans, all samples were tubulointerstitial tissue, and the dataset contained both control and experimental groups. Data from repeated renal biopsies were excluded from the analysis. The GSE32591, GSE113342, and GSE200306 datasets including 35 controls and 91 LNs were obtained as integrated microarray datasets after screening.

Differentially Expressed Gene (DEG) Assay and Integrated Microarray Dataset Analysis

The three included datasets were merged based on platform annotation. As these datasets were obtained from different platforms, exhibited batch effects, we used the "sva" package to mitigate batch effects. The package "FactoMineR" and "factoextra" were used for principal component analysis (PCA). DEGs were screened based on the fold change (FC) of gene expression between the LN and normal groups, calculated using the "Limma" package in R with |Log2FC| > 1 and adjusted p value< 0.05.

Functional Enrichment Analysis

To identify the potential roles of DEGs, we performed gene ontology (GO) and Kyoto Encyclopedia of Genes and Genomes (KEGG) analyses using the "clusterProfiler" package in R, and $p < 0.05$ was considered statistically significant.

Screening of Candidate Diagnostic Genes

Two machine learning algorithms, including least absolute shrinkage and selection operator(LASSO) logistic regression and support vector machine-recursive feature elimination(SVM-RFE), were utilized to screen core genes. The "glmnet" package was utilized to apply the LASSO algorithm, obtained the best λ by ten cross-validations finally gained the core genes based on the best λ. The package "e1071" was used in the SVM-RFE algorithm, Initially, the importance of the candidate diagnostic genes were ranked based on the feature weights of the support vectors. Then the cross-validation error was estimated using ten-fold cross-validation. At last, candidate genes were identified after taking the intersection of genes obtained by LASSO and SVM-RFE.

Analysis of Infiltrating Immune Cells

CIBERSORT is a tool for deconvolution of expression matrices of human immune cell subtypes based on the principle of linear support vector regression. Both chip expression matrix and sequencing expression matrix can be analyzed by this tool, estimating the infiltration of immune cells using RNA-sequencing data.[13] In our study, the CIBERSORT algorithm was used to compare the relative proportions of different immune cells in the normal and LN samples. As the computational analysis was completed, CIBERSORT results $p<0.05$ were selected to filter the samples for differentially infiltrating analysis. The relationship between bio diagnostic markers and immune cells were analyzed with Spearman correlation coefficient. For those with $p<0.05$, the results were visualized using the "ggplot2" package.

Patients and Human Kidney Biopsy Specimens

Three cases of LN who underwent renal biopsy diagnosis from August 2022 to December 2023 in the First Affiliated Hospital of Fujian Medical University were selected; normal control kidney samples were also obtained from the nontumor regions adjacent to renal cancerous tissue from three patients with solitary renal cell carcinoma. The corresponding information of clinical and renal biopsy were collected, including gender, age, estimated glomerular filtration rate of serum creatinine, 24-hour urinary protein quantification, the degree of hematuria (the hematuria scale was used as follows: 0 if <5 RBCs per high-power field (HPF), 1 if 6–20 RBCs/HPF, 2 if 21–50 RBCs/HPF, and 3 if 451 RBCs/HPF),[14] and renal pathology reports. Renal pathological findings were reviewed independently by two pathologists.

Mice Models

For the animal experiments, both MRL/lpr and C57BL/6 mice served as normal controls (Shanghai SLAC Laboratory Animal Co.,Ltd) aged 8–10 weeks were choosed. The mice were housed in a specific pathogen-free facility, and kept in an environment with a constant temperature of 25 °C and relative humidity of 40–60%. Conventional fodder was not restricted. At the age of 20 weeks, the mice were euthanized and blood and kidney tissues were collected for subsequent experiments.

Immunofluorescence Staining

Immunohistochemical staining was performed according to a routine protocol. Briefly, gradient dewaxing, hydration of the kidney tissue sections, and antigen repair were performed. Thin sections were incubated with the following primary

antibodies: anti-MX1 (1:200, ab222856, Abcam); anti-EGR1 (1:200, ab300449, Abcam); anti- IFI204 (1:200, ab307201, Abcam); anti-IFI16 (1:200, ab169788, Abcam); anti-Lrp2/megalin (1:200, ab184676, Abcam); and anti-F4/80 (1:200, ab16911, Abcam) for 4 h at room temperature, and then stained with Alexa Fluor 488 (Abcam), Alexa Fluor 568 (Abcam), and Alexa Fluor 647 (Abmart). DNA was labeled with 4′,6-diamidino-2-phenylindole (Invitrogen).

Isolation of Primary Renal Tubular Cells

The mouse primary proximal renal tubular cells were isolated as described previously.[15] The renal cortices were dissected, transferred to Dulbecco's modified Eagle medium with 0.75 mg/mL collagenase D (Roche, Germany), and digested at 37 °C for 30 min. The suspension was filtered (pore size, 100 μm) and resuspended in Hanks' balanced salt solution. The proximal tubule was then centrifugally enriched on a self-forming Percoll gradient at 4 °C. Freshly isolated proximal tubule fragments were collected.

Western Blotting

Proteins were extracted from primary proximal renal tubular cells, and the protein concentration was determined using the BCA assay. A total of 50μg protein per lane was separated by gel electrophoresis and transferred to a polyvinylidene fluoride membrane. The proteins were incubated overnight at 4 °C with the following antibodies: anti-MX1 (1:1000, ab222856, Abcam); anti-EGR1 (1:1000, ab300449, Abcam); anti-IFI204 (1:1000, ab307201, Abcam); and anti-GAPDH (mouse monoclonal; 60004, Proteintech). The membrane was washed and the secondary antibody (1:5000) added to the proteins and incubated for 1 h at room temperature. Finally, an electrochemiluminescence system was used for color development, and an image analysis system was used to scan grayscale images.

Quantitative Real-Time Polymerase Chain Reaction (RT-qPCR)

Total RNA was extracted from mouse renal tubular cells using TRIzol reagent combined with organic solvents. RNA was reverse-transcribed into cDNA using a reverse transcription kit (R333-01; Vazyme). RT-qPCR was performed using QuantStudio 5 (Thermo Fisher Scientific) with the SYBR qPCR mix as the fluorescent dye. The following primers were obtained from Metabion (Martinsried, Germany): EGR1 sense: **CGTCCTGTTCCCTTTGACTT**, antisense: **GCATGTGATGGAGAGGATACTG**; MX1 sense: AGATGAGGAGAGAGGAGCTATG, antisense: CCAGTACATCCTCCTGACAAAG; IFI204 sense: TGACTTAGCTGCCTACCTACT, antisense: GCTGAGCCTTCCTGGATATTT; β-actin sense: GGCTGTATTCCCCTCCATCG, antisense: CCAGTTGGTAACAATGCCATGT. β-actin was used as an internal reference. The relative mRNA expression of the target gene was calculated using the $2^{-\Delta\Delta CT}$ method.

Statistical Analysis

Continuous variables were described as mean±SD, or minimum and maximum values. A *t*-test was used for comparisons between groups. Images were drawn using GraphPad Prism version 8.0. Statistical analyses were performed using IBM SPSS version 26.0. Statistical significance was set at $p < 0.05$.

Results

Identification of DEGs in LN Tubules

According to the screening criteria, eliminating batch effects, then following a principal component analysis (PCA) on the combined samples: normal and LN samples were clearly separated in the PCA plot, suggesting a significant individual differences (Supplementary Figure 1). The DEGs in the interpreted data were analyzed using the "Limma" package. Overall, 17 DEGs were identified, of which 11 were markedly upregulated, including IFI16, MX1, STAT1, etc; and 6 downregulated, including EGR1, RORC, KIT, FKBP5, MME and ZBTB16 (Figure 1 and Table 1).

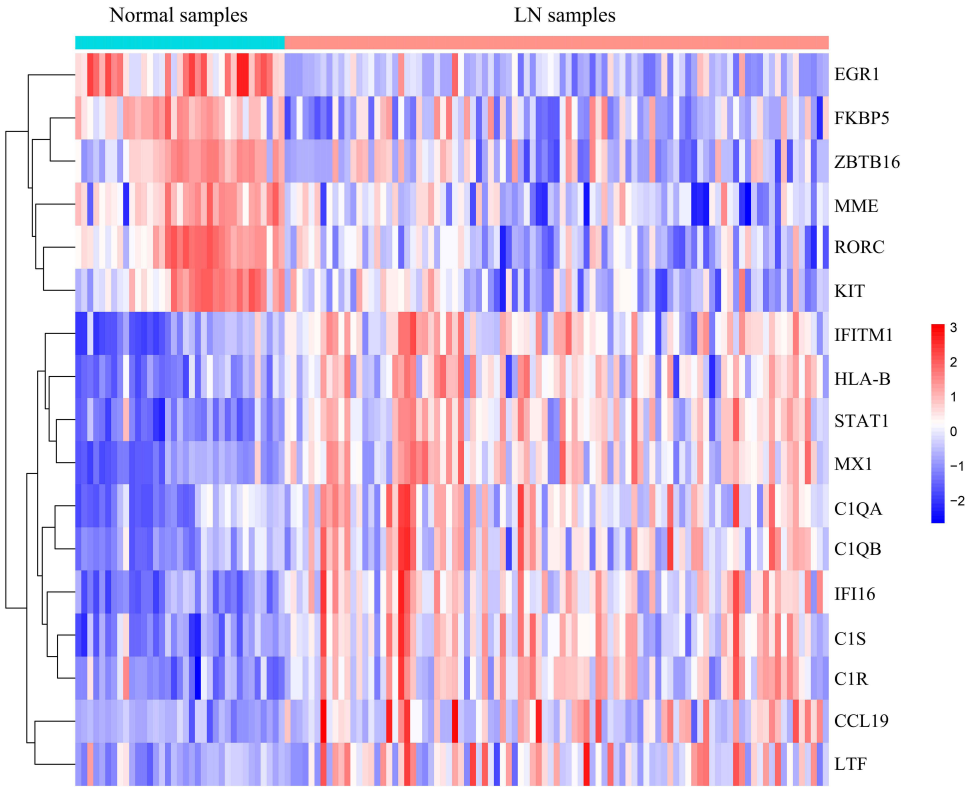

Figure 1 Heatmap displaying the expressions of the DEGs between normal and LN specimens. Blue corresponds to lower gene expression and red to higher gene expression.

Gene Ontology and Kyoto Encyclopedia of Genes and Genomes Analysis

To investigate the biofunction of the 17 DEGs in LN, we performed GO and KEGG analyses using the "ClusterProfile" R package. GO analysis revealed that these genes were predominantly enriched in such biological processes (BP) as

Table 1 The Different Expression of Key Genes in Renal Tubule Interstitium. Lupus Nephrities Samples versus Normal Samples

Gene	logFC	AveExpr	t	adj.P.Val
STAT1	1.62511912	7.04963334	11.1121115	4.45E-18
IFI16	1.25193132	5.39438722	10.2118153	3.48E-16
MX1	2.13768387	7.53507988	10.1197619	4.69E-16
IFITM1	1.49863119	8.63199944	9.14423912	7.10E-14
C1S	1.47194375	6.28769723	9.08008979	9.03E-14
HLA-B	1.08753692	10.0127735	8.22714105	8.16E-12
C1R	1.37578905	6.75021357	7.63385531	1.69E-10
C1QA	1.06849732	6.07939708	6.9367449	4.01E-09
C1QB	1.13522658	7.30220792	6.63157413	1.47E-08
CCL19	1.19935296	5.40073753	5.76855987	6.51E-07
LTF	1.30331154	7.17258061	4.85068363	2.88E-05
EGR1	−2.1355066	7.59188425	−11.101703	4.45E-18
RORC	−1.4040485	6.86208184	−9.4486639	1.48E-14
KIT	−1.4412948	5.48223392	−7.2859872	7.65E-10
FKBP5	−1.7841981	6.74179274	−6.7110796	1.06E-08
MME	−1.1136026	8.96159888	−6.5835837	1.81E-08
ZBTB16	−2.1903908	6.10526613	−5.928683	3.76E-07

Abbreviations: logFC, log2 fold change; AveExpr, average expression of a gene in all samples; t, refers to statistics.

adaptive immune responses based on the somatic recombination of immunoglobulin superfamily domain immune receptors, complement activation by classical pathways. In terms of cellular components (CC), these genes were chiefly enriched in blood microparticles. Regarding the molecular functions (MF), these genes were characterized by amide binding, serine-type peptidase activity, and histone acetyltransferase binding. KEGG enrichment analysis revealed their associations with pathways such as COVID-19, pertussis, complement and coagulation cascades, staphylococcus aureus infection, and SLE (Figure 2A and B).

Determination and Validation of Diagnostic Markers

We used two different algorithms, LASSO regression and SVM-RFE, to screen for the underlying biological markers. Seven DEGs were identified using LASSO regression as diagnostic markers of LN tubulointerstitial injury, and eight DEGs were identified using the SVM-RFE algorithm. We used the intersection of the two algorithms and identified seven core genes: *EGR1, IFI16, MX1*, RORC, *IFITM1, KIT*, and *FKBP5*. These seven genes may be key to the progression of LN-associated tubulointerstitial injury (Figure 3A and B, and veen diagram is shown in Supplementary Figure 2).

Validation of Core Gene Expression and Diagnostic Efficacy

Expression of *FKBP5, EGR1, KIT*, and *RORC* in LN samples was significantly lower than that in healthy samples, whereas the expression of *IFI16, IFITM1*, and *MX1* was considerably upregulated in LN samples. To further explore the diagnostic value of these core genes, we performed a receiver operating characteristic (ROC) analysis. The seven genes exhibited strong LN screening capabilities, including *IFI16* (area under the ROC curve [AUC] = 0.948), *FKBP5* (AUC = 0.827), *EGR1* (AUC = 0.925), *KIT* (AUC = 0.825), *RORC* (AUC = 0.906), *MX1* (AUC = 0.930), and *IFITM1* (AUC = 0.910) (Figure 4A-F and Supplementary Figure 3A-D and Supplementary Figure 4A-D).

IFI16, EGR1 and MX1 Were Related to Immunocyte Infiltration Levels

Abnormal activation of immune cells is an important feature of LN. Using the CIBERSORT algorithm, we investigated the infiltration characteristics of immune cells in the tubulointerstitium of LN and the interrelationships between immune cells (Figure 5A and B). We also observed significant dysregulation in the proportions of regulatory T cells, γδ T cells, M1 macrophages, activated mast cells, and eosinophils between the normal and LN samples. In addition, we explored the relationship between the DEGs and immune infiltration levels. *IFI16* was associated with γδ T cells, $CD8^+$ T cells, plasma cells, resting mast cells, activated mast cells, M1 macrophages, eosinophils, and activated dendritic cells. *EGR1* was correlated with monocyte and M1 macrophage populations. *MX1* was associated with $CD8^+$T cells, plasma cells, resting mast cells, activated mast cells, M1 macrophages, and eosinophils. These findings suggest that *IFI16, EGR1*, and

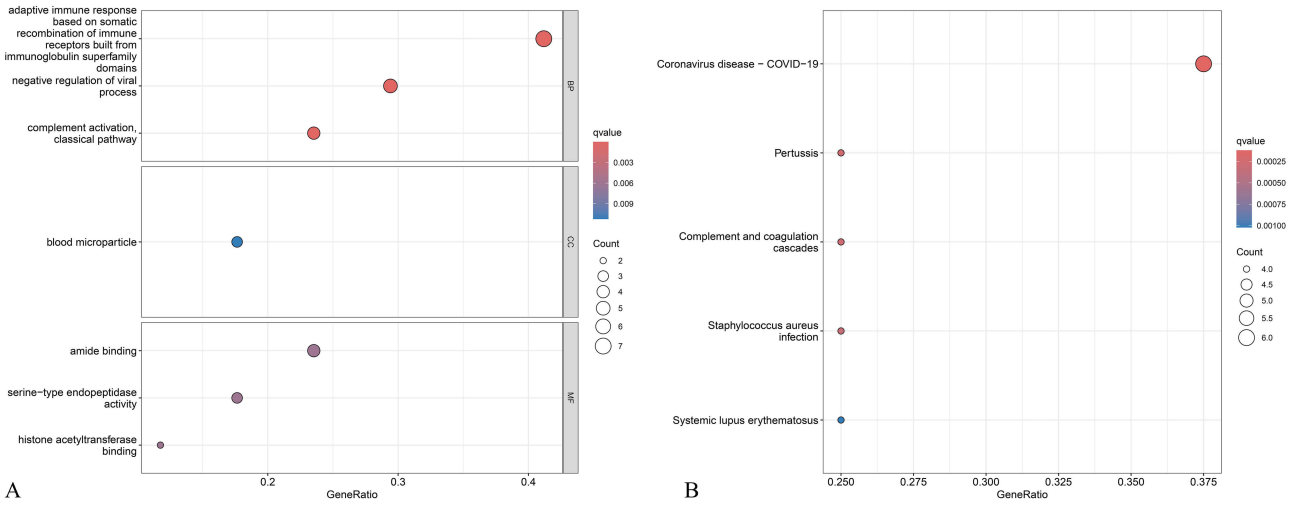

Figure 2 GO and KEGG enrichment analysis of DEGs related to LN. (**A**) Bubble plot of enriched GO terms showing DEGs; (**B**) Bubble plot of enriched KEGG pathways showing DEGs. A redder color and a larger bubble denote a more significant difference.

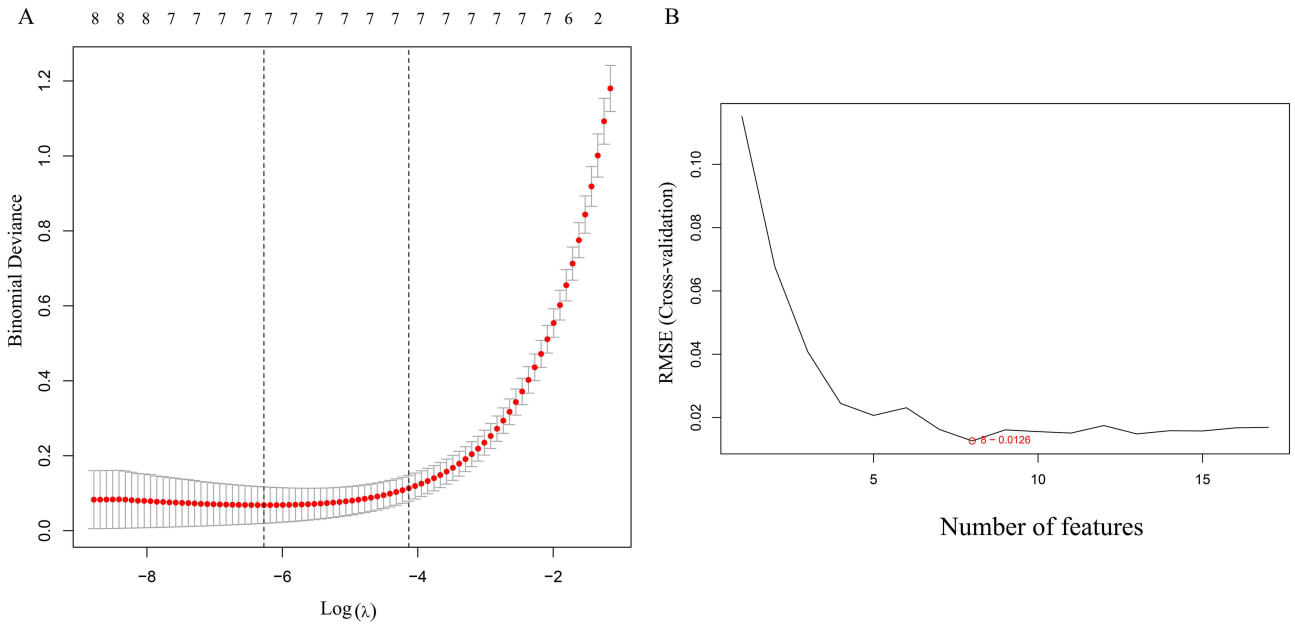

Figure 3 Selection of diagnosis marker candidates for LN. (**A**) Tuning feature screening in the LASSO model. The selection process of the optimum value of the parameter λ in the Lasso regression model by cross-validation method, The solid vertical lines represent the partial likelihood deviance SE, and the number of genes (n = 7) corresponding to the lowest point of the curve is the most suitable for LASSO. (**B**) A plot of biological marker screening via the SVM-RFE arithmetic. The ordinate represents the error rate of the curve change after ten cross-validation, and the number of genes (n = 8) indicates the lowest error rate which is the most suitable for SVM-RFE.

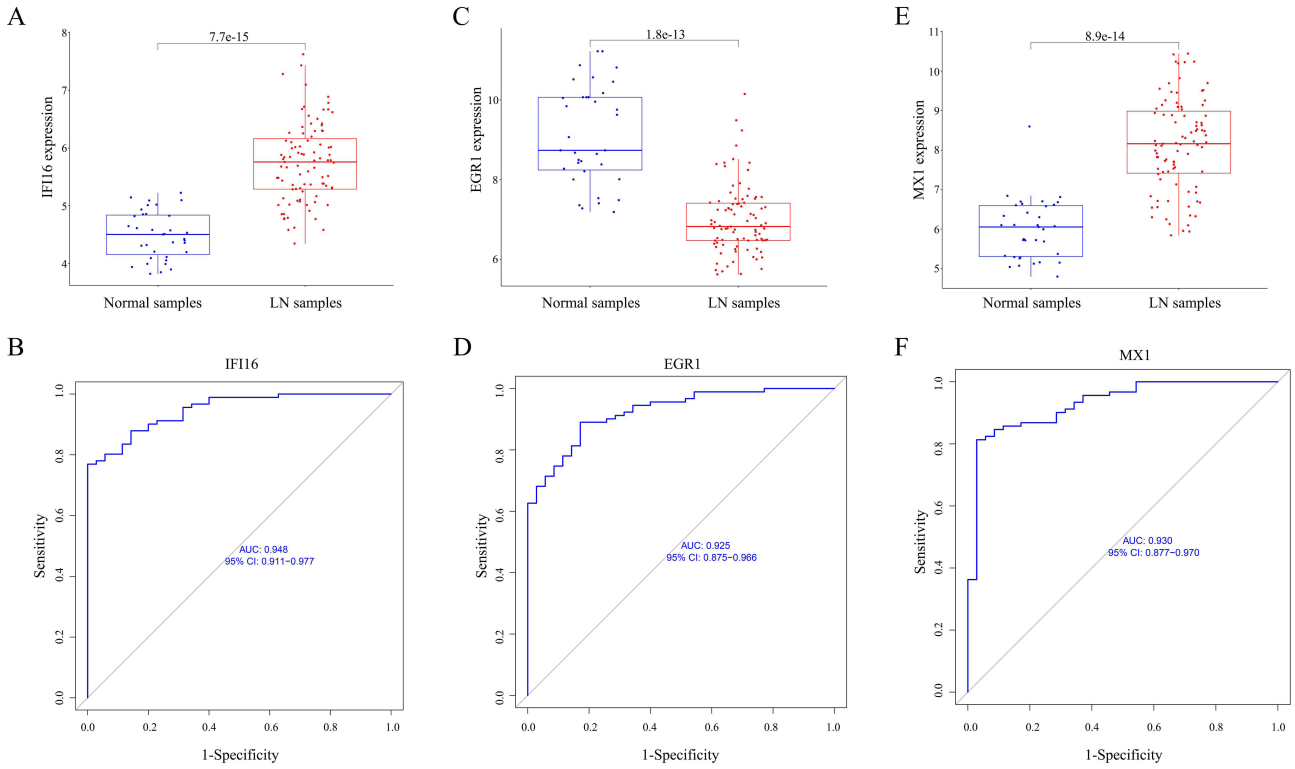

Figure 4 The expression and diagnosis significance of *IFI16*, *EGR1* and *MX1* in LN. (**A**) *IFI16* expression was distinctly upregulated in LN samples; (**C**) *EGR1* expression was distinctly downregulated in LN samples; (**E**) *MX1* expression was distinctly upregulated in LN samples. (**B**/**D**/**F**) Receiver operating characteristic (ROC) curves for *IFI16*, *EGR1* and *MX1* in LN. Normal samples n=35, LN samples n=91.

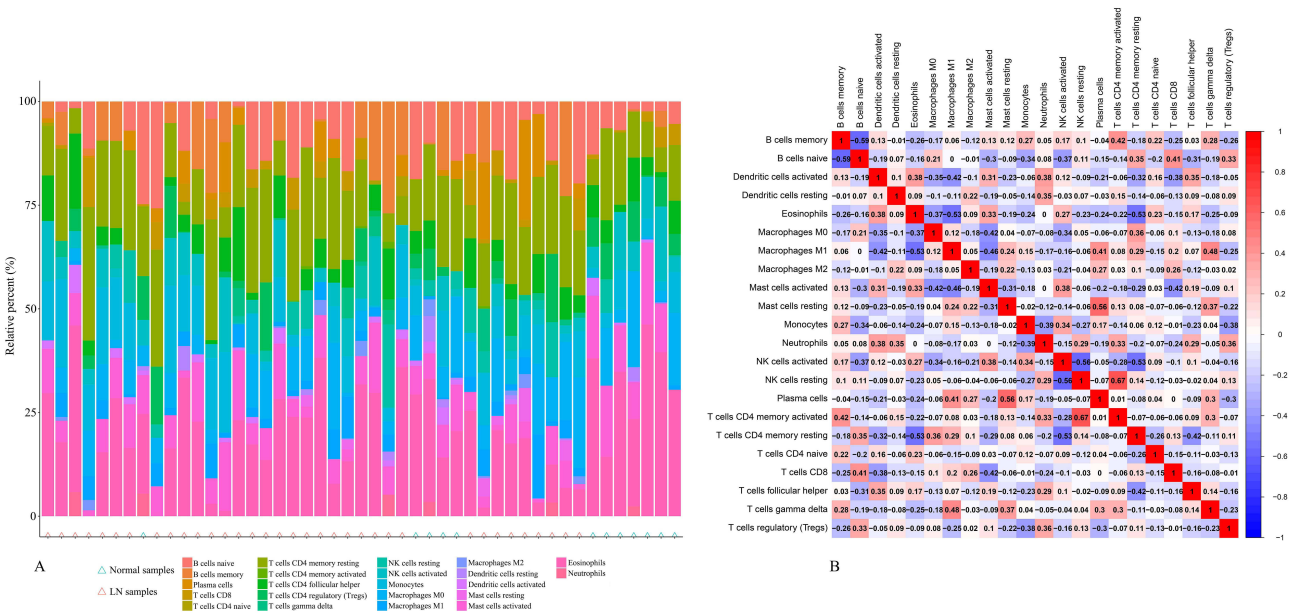

Figure 5 Distribution of 22 kinds of immune cells and heatmap of correlations between 22 immune cell subtypes. (**A**) Bar charts of 22 immune cell proportions in normal and LN tubulointerstitium tissues; (**B**) Heatmap of correlations between 22 immune cell subtypes. Both horizontal and vertical axes show immune cell subtypes, and the values inside represent the correlation coefficients of immune cells. Red represents positive correlation and blue represents negative correlation.

MX1 play immunomodulatory roles in tubulointerstitial injury in LN (Figure 6A-D). Nevertheless, we found no obvious association between other four genes - RORC, IFITM1, KIT and FKBP5 - and immune cell infiltration.

IFI204, EGR1, and MX1 Significantly Increased in Tubules in MRL/Lpr Mice

To further verify our findings, we selected both MRL/lpr and controlled mice. First, we compared the renal pathology of the two groups, MRL/lpr mice showed obvious tubulointerstitial inflammation and injury (Figure 7A and B). As we know renal tubular epithelial cells, the main structural cell group of the kidney, are actively involved in tubulointerstitial inflammation and injury. Then we extracted tubular epithelial cells to examine *IFI204* (human homologous protein is *IFI16), EGR1*, and *MX1* expression. Consistent with our previous results, the mRNA and protein expression of *IFI204*, and *MX1* were distinctly upregulated in MRL/lpr mice. However, the result of *EGR1* was inconsistent with the previous findings, both the mRNA and protein expression of *EGR1* were markedly increased in MRL/lpr mice (Figure 7C-F). These results provide strong evidence of the involvement of *IFI204, EGR1, and MX1* in LN-associated tubulointerstitial injury.

Multiplex Immune Fluorescence Staining of Renal Tubules Fields IFI16 or IFI204, EGR1 and MX1 Expression, and Co-Localisation with Macrophage in LN

To clarify the expression of *IFI16* or *IFI204, EGR1*, and *MX1* in the tubulointerstitium of LN, we selected patients with LN and renal cancer patients (the nontumor regions adjacent to renal cancerous tissue) as control for cross-comparison. Then we performed multiple immunofluorescence staining for the target proteins and tubular. We can see that the expression of target proteins were significantly higher in the tubular interstitium of patients with LN (whose clinical characteristics were aged from 39 to 53, the results of hematuria was 1.33±1.53, dominant proteinuria (4.88±3.35 g/24h), serum creatinine (umol/L) was 72.3±29.1, hypocomplementemia; and histopathological characteristics of the kidney biopsy samples showed that glomerulosclerosis (%) was 0–33.3, and tubulointerstitial fibrosis (%) was 8–20). We also can see that the number of infiltrating macrophages increased in the tubular interstitium of patients with LN. Additionally, target proteins co-localized well with macrophage in tubulointerstitial areas. Similar phenomena was also found in MRL/lpr mice than in controlled groups. (Figure 8A-C and Figure 9A-C).

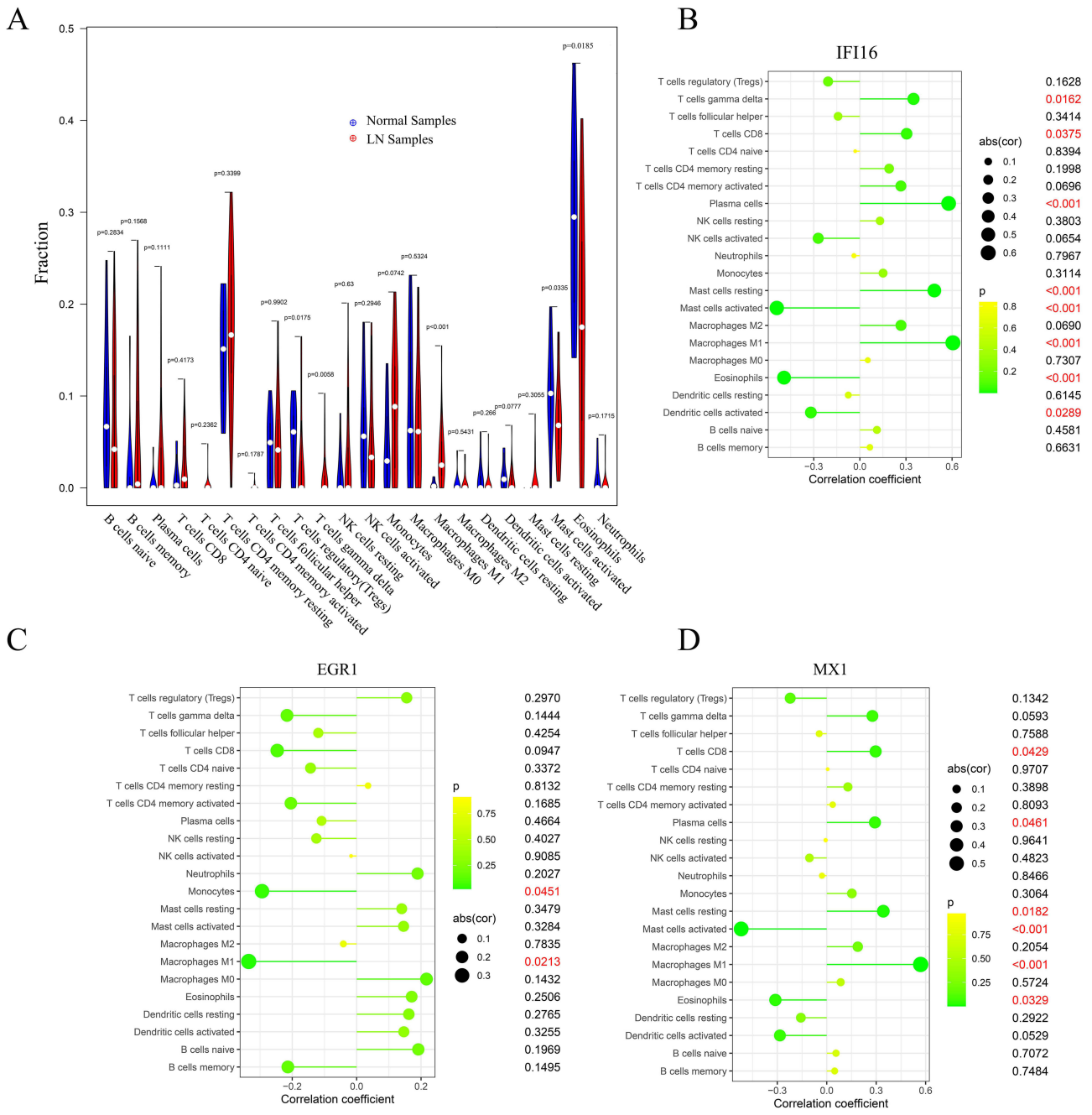

Figure 6 Immune cell infiltration analysis of lupus nephritis. (**A**) Violin diagram of 22 types of immune cells between normal and LN specimens. Correlation of core genes *IFI16* (**B**), *EGR1* (**C**), *MX1* (**D**) with infiltrating immune cells; the vertical ordinate represents the name of the immune cell and the abscissa represents the correlation coefficient; the circle size represents the absolute value size of the correlation coefficient.

Discussion

SLE is characterized by an inflammatory response and immune system dysfunction. LN mainly manifest as glomerular immune complex deposits, but up to 40% of LN involve the tubulointerstitium and/or vessels.[16] Tubulointerstitial injury is characterized by varying degrees of inflammatory cell infiltration, tubule atrophy, and interstitial fibrous scar formation. Studies have shown that tubulointerstitial inflammation can better predict poor renal prognosis than glomerular injury.[17,18] The number of interstitial infiltrates is typically used to evaluate tubulointerstitial inflammation. Tubulointerstitial injury is thought to begin with an inflammatory process that, if not attenuated, can promote interstitial fibrosis and tubulointerstitial atrophy, which are irreversible structural changes.[9] However, little is known about the

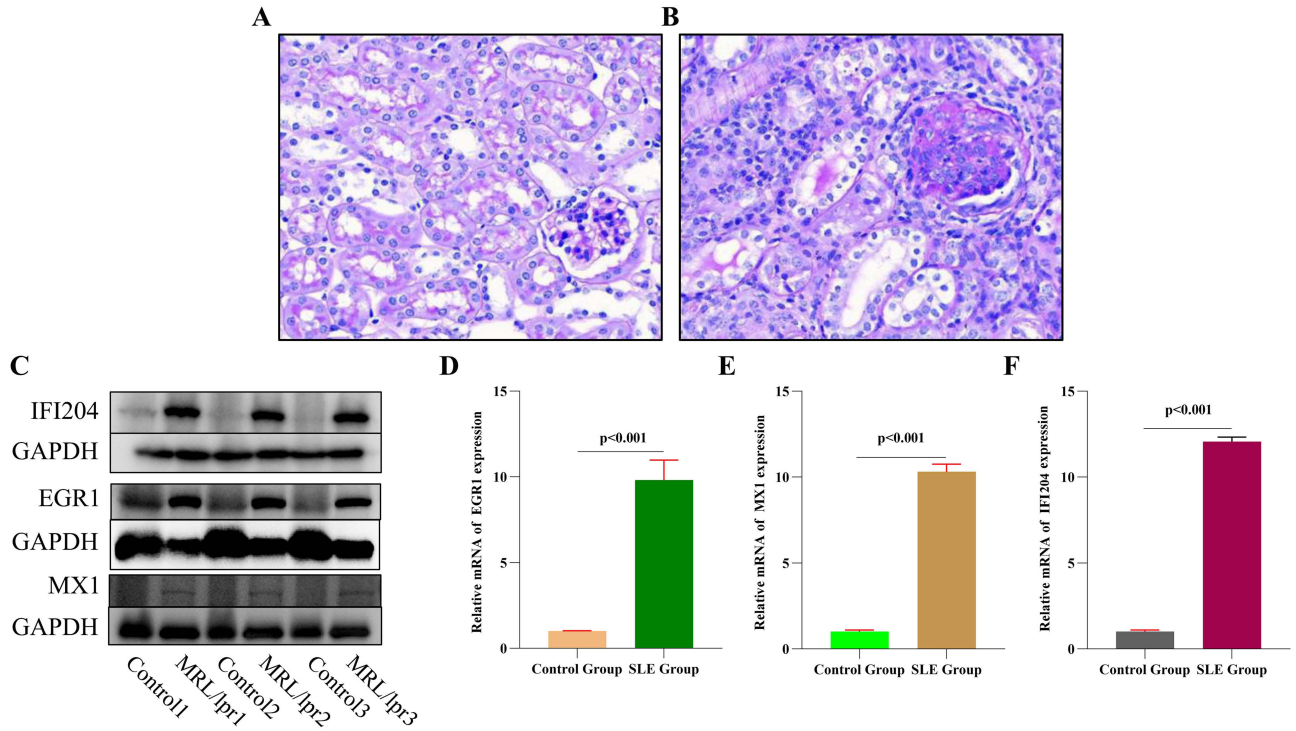

Figure 7 Renal pathology and expression of IFI204, EGR1 and MX1 in tubular epithelial cells in LN. (**A**) HE staining of control mice kidney tissue sections. (**B**) HE staining of MRL/lpr mice kidney tissue sections. (**C**) The protein of IFI204, EGR1 and MX1 levels were examined in protein extracts from tubular epithelial cells of MRL/lpr or C57BL/6 mice, and (**D-F**) RT-qPCR for the levels of mRNA levels of *EGR1*, *MX1* and *IFI204* of tubular epithelial cells isolated from MRL/lpr or C57BL/6 mice. All data were shown as mean ± SD.

specific cell types and mechanisms involved in tubulointerstitial alterations in LN. It is important to fully understand the tubulointerstitial immune infiltration of LN and the possible regulatory factors involved in the improvement of renal prognosis. Our results indicated that the LN tubulointerstitial region was enriched in a variety of cells, such as M1 macrophages, and that local aggregation of M1 macrophages was significantly correlated with tubulointerstitial IFI16, EGR1 and MX1 expression. Tubular epithelial cells are resident cells of the kidney and are closely related to various pathological processes in acute and chronic kidney diseases. They can actively regulate the responses of tubulointerstitial immune cells (such as dendritic, T, and B cells) through the production of soluble factors (such as pro-inflammatory cytokines and chemokines) and the expression of co-stimulatory and co-inhibitory molecules on the cell surface. For example, plasma cells that secrete anti-dsDNA antibodies in mice with LN are primarily present in the renal tubulointerstitium. In addition, $CD11C^{+}$ macrophages infiltrating the tubulointerstitium can trigger IL-6-mediated expression and apoptosis of fibronectin in tubular epithelial cells.[12,19]

Macrophages, T cells, B cells, and dendritic cells constitute the main diverticula of interstitial infiltration in LN kidneys, with macrophages accounting for the largest proportion (approximately 50%).[20] Previous studies have shown that increased renal macrophage infiltration is associated with poor renal survival.[21,22] Macrophages interact with tubular epithelial cells and the extracellular matrix; damage the endothelial/epithelial barrier; produce a variety of cytokines, chemokines, and reactive oxygen species; promote renal inflammation and renal interstitial fibrosis; and participate in the development of chronic kidney disease.[23–25] Therefore, it is critical to identify and intervene in the regulatory factors that affect the local infiltration of macrophages.

In our study, we found, for the first time, that the expression of IFI16 mRNA and protein in the tubular epithelial cells of MRL/lpr mice was significantly higher than that in control mice. We also found that the expression of IFI16 in the tubulointerstitium was related to the local infiltration of macrophages. Previously, Wang et al used multiplexed immunofluorescence staining to show that IFI16 co-localizes well with podocytes, mesangial cells, and glomerular endothelial cells in patients with LN.[26] Our results suggest that IFI16 is localized in the tubulointerstitial region.

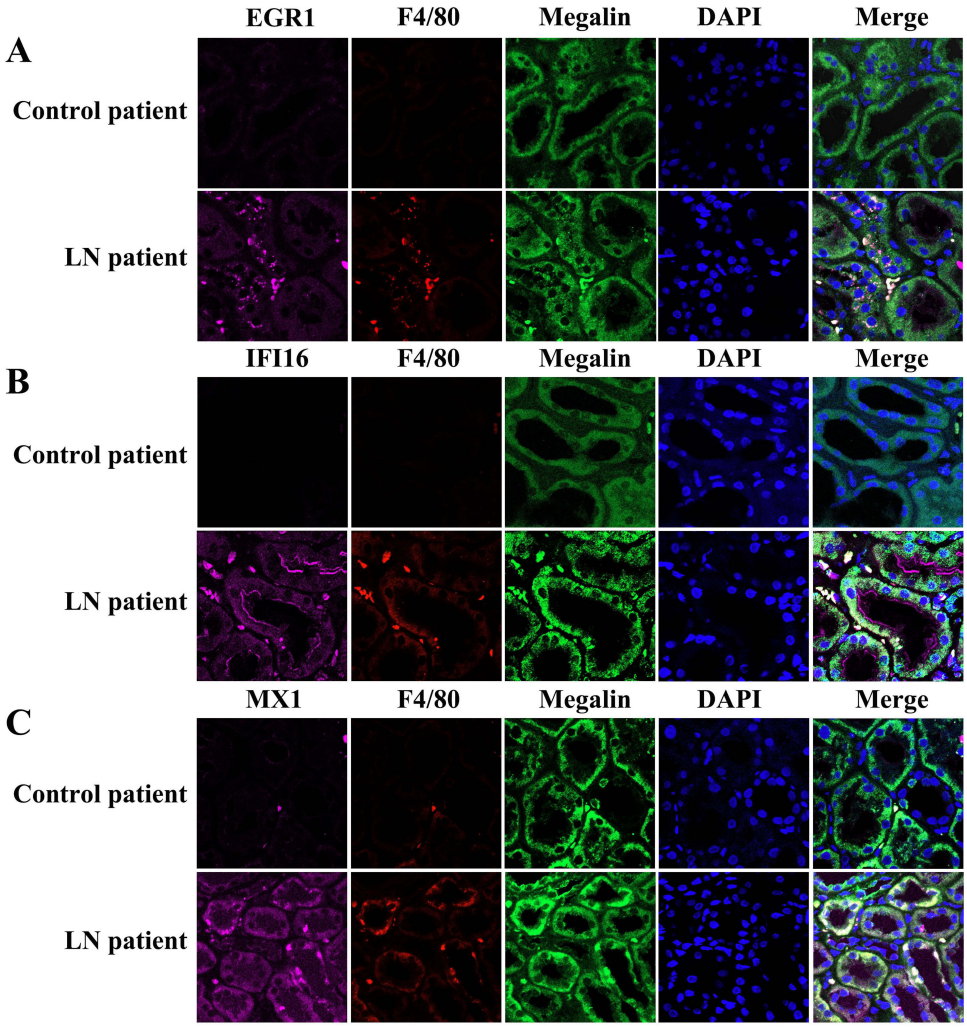

Figure 8 Expression of target protein in renal tubular with LN patients. Co-localisation of target proteins (pink) (**A)** EGR1, (**B)** IFI16 and (**C)** MX1, F4/80 (red) (marker of macrophage), and Megalin (green) (marker of the renal tubules). DAPI was used for nuclear staining. LN, lupus nephritis; DAPI, 4′,6-diamidino-2-phenylindole.

IFI16 is an HTN-200 protein with a DNA-binding domain containing 200 amino acids at the C-terminus and a PYRIN domain at the N-terminus. Its mouse homologue is IFI204.[27,28] IFI16 is widely distributed in the nucleus and cytoplasm and can be used as a DNA sensor in both the nucleus and cytoplasm. Studies have found that IFI16 activates the NF-kB complex to trigger the expression of pro-inflammatory adhesion molecules (ICAM-1) and chemokines (CCL4,CCL5,CCL20, etc)., recruiting immune cells to play an immunomodulatory role. During viral infection, IFI16 forms an inflammasome complex by binding to the viral dsDNA, which is then transported into the cytoplasm. IFI16 mediates pyroptosis by inducing the release of proinflammatory interleukins and the activation of caspase-1. It can also mediate IFN-β production via the STING-TBK1 pathway. In addition, IFI16 overexpression activates caspase-2 and caspase-3 to induce apoptosis.[29–32] IFI16 is an important inflammatory mediator in autoimmune diseases. Recent studies have found that the expression of IFI16 in patients with SLE is positively correlated with the SLE disease activity index score and anti-ds-DNA antibody titers but negatively correlated with C3/C4 hypocomplementemia. Patients with high IFI16 expression are more likely to develop eye diseases.[33] In the present study, increased expression of IFI16 in the tubulointerstitial region distinctly increased the local infiltration of macrophages; however, the specific mechanism remains unclear. Previous studies have suggested that overexpressed IFI16 can induce inflammasome activation to produce IL-1β, which mediates the maturation, migration, and local proliferation of macrophages.[34] However, further research is required to elucidate this mechanism.

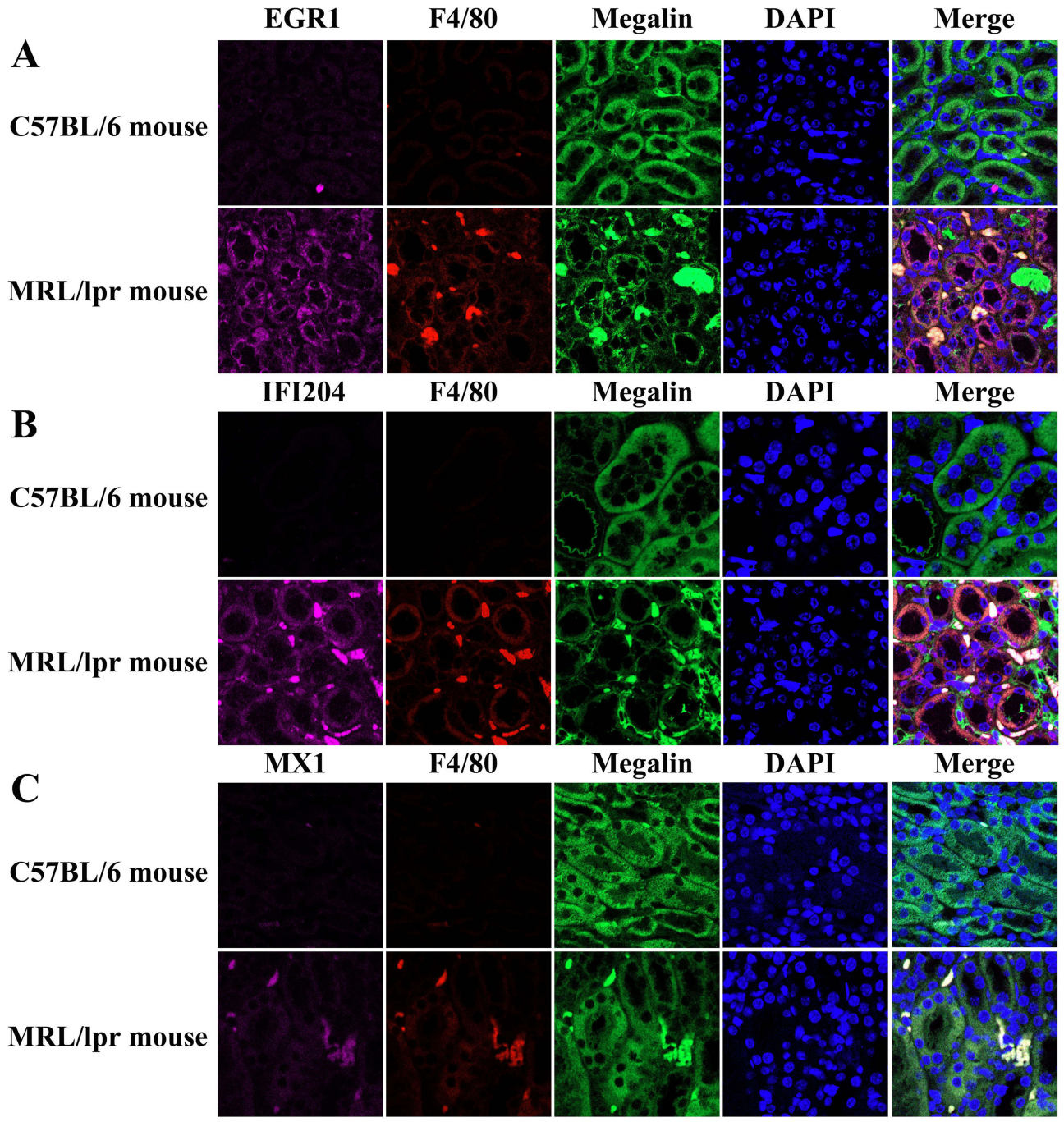

Figure 9 Expression of target protein in renal tubular within MRL/lpr. Co-localisation of target proteins (pink) (**A**) EGR1, (**B**): IFI204 and (**C**): MX1, F4/80 (red) (marker of macrophage), and Megalin (green) (marker of the renal tubules). DAPI was used for nuclear staining. LN, lupus nephritis; DAPI, 4′,6-diamidino-2-phenylindole.

Early Growth response factor 1 (EGR1) is also known as EGR-1, EGR1 gene is located in the 5q23-31 region of human chromosome, which contains an activation regulatory region, an inhibitory regulatory region and three Cys2-His2 subclass zinc finger structures.[35]

EGR1 is widely expressed in a variety of cells, its expression is induced by environmental stimuli associated with injury and stress, which include neurotransmitters, cytokines, endotoxins, hypoxia, oxidative stress, etc. And it is involved in cell proliferation, differentiation, apoptosis, migration and inflammatory reaction.[36]

Several potential mechanisms of Egr-1 in the regulation of inflammation and fibrosis have been proposed. For example, Egr-1 can enhance the expression of tumor necrosis factor-α (TNF-α), NF-κB, and TGF-β because the promoters of these genes all contain Egr-1 binding sites. Egr-1 also regulates post-transcriptional activity of NF-κB by direct interaction with the NF-κB subunit, or indirectly by inducing activators of NF-κB such as TNF-α. Studies have shown that upregulation of EGR1 expression in tubulointerstitial nephritis can promote the production of proinflammatory cytokines and chemokines in renal tubular cells, and aggravate renal failure; when EGR1 deficiency attenuated the transcriptional activity of NF-ƙβ, inflammatory factors expression, immune cell infiltration and renal tubule injury.[37] Importantly, EGR1 is also of clinical significance, In patients with glomerulonephritis such as lupus nephritis, the expression of EGR1 in podocytes is significantly increased and correlated with the formation of cell/fibrocyte crescent, proteinuria, and mRNA levels of uropodocytes, suggesting that EGR1 is a pathological marker of podocyte injury in glomerulonephritis.[38] Different from the results of bioinformatics analysis, we have verified that the expression of EGR1 in renal tubule cells in LN is significantly increased. It should be noted out that, our research is based on the GEO database, which is a database for secondary mining and analysis of previously published data sets; in addition, the sample size of the datasets available to us is small, which may cause the deviation between the analysis conclusion and the verification result.

The MX1 gene in mice is located on chromosome 16, a region that is syntenic with the long arm of human chromosome 21, it contains 17 exons extending over 33 kb and encodes a large GTPase, MxA.MX1 gene expression is induced by type I (α/β) and III (λ) IFNs.[39,40] Elevated levels of MX1 induce an adaptive immune response, which leads to a breakdown of self-antigen tolerance. MX1 expression has also been reported to play an important role in apoptosis and cytokine-mediated cell signaling and in lupus nephritis.[41]

For lupus patients, the expression of MX1 in peripheral blood was significantly higher than that of ordinary people, and the high expression of MX1 was significantly correlated with hypocomplementemia and lupus activity.[42–44] In addition, the expression of MX1 in the glomeruli and renal tubules fields of lupus patients was significantly increased, while the expression of MX1 in the kidneys of LN patients treated with immunosuppressants was also remarkably decreased compared with those from immunosuppressant naïve patients.[45] The present study also found that compared with the control mice, the expression of MX1 in renal tubular epithelial cells of lupus nephritis was significantly increased; multiple immunofluorescence staining showed that MX1 was increased in the renal tubular area of LN patients, and MX1 expression was correlated with macrophage infiltration. The effect of MX1 on tubular epithelial cells of LN is not fully understood at present, and more studies are needed in the future.

Limitations

Our study had some limitations. First, we did not elucidate the underlying mechanism between the target protein and immune cell infiltration. Second, we failed to collect more patients data to explore the correlation between these target proteins and clinical indicators in LN patients. Third, the correlation between bioinformatically determined LN biomarkers and immune cell infiltration needs to be confirmed in studies with large sample sizes. Fourth, the different clinical stages of the patients with LN may have caused selective deviations in the analysis results. Fifth, we did not further distinguish between M1 and M2 macrophages during the verification stage. Sixth, after verification of animal and human tissue samples, differences were found within EGR1 versus bioinformatics analysis, and further studies are needed to confirm this.

Conclusions

IFI16, EGR1 and MX1 are upregulated in LN tubular epithelial cells, associated with immune infiltration, and are considered key biomarkers of tubulointerstitial injury in LN. Our study showed that they are involved in the development of LN, providing new insights into the underlying mechanisms of the disease and as a potential diagnostic and therapeutic target for LN.

Data Sharing Statement

The data that support the findings of this study are available from the corresponding author upon reasonable request.

Ethics Approval and Consent to Participate

The present experiments were accomplished in compliance with the Declaration of Helsinki, all participants provided informed consent prior to study inclusion, and all the animal experiments were performed according to the "China Guide for the Protection and Use of Laboratory Animals". This research was approved by the Ethics Committee of Fujian Medical University (No.IACUC FJMU 2024-0197), and of the First Affiliated Hospital of Fujian Medical University (No.MRCTA, ECFAH of FMU [2022]454).

Funding

This work was supported by Natural Science Foundation of Fujian province (2023J01583), Joint Funds for the innovation of science and Technology of Fujian province (2021Y9116), Fujian Provincial Health Technology Project (No. 2021ZQNZD004). Yanfang Xu was supported by Outstanding Young Talents Program of the First Affiliated Hospital of Fujian Medical University (YJCQN-A-XYF2021).

Disclosure

The authors declared that they have no conflicts of interest to disclose.

References

1. Kolios AGA, Tsokos GC. Skin-kidney crosstalk in SLE. *Nat Rev Rheumatol*. 2021;17(5):253–254. doi:10.1038/s41584-021-00588-0
2. Davidson A. What is damaging the kidney in lupus nephritis? *Nat Rev Rheumatol*. 2016;12(3):143–153. doi:10.1038/nrrheum.2015.159
3. Anders HJ, Saxena R, Zhao MH, et al. Lupus nephritis. *Nat Rev Dis Primers*. 2020;6(1):7. doi:10.1038/s41572-019-0141-9
4. Bajema IM, Wilhelmus S, Alpers CE, et al. Revision of the international society of nephrology/renal pathology society classification for lupus nephritis: clarification of definitions, and modified national institutes of health activity and chronicity indices. *Kidney Int*. 2018;93(4):789–796. doi:10.1016/j.kint.2017.11.023
5. Yu F, Haas M, Glassock R, et al. Redefining lupus nephritis: clinical implications of pathophysiologic subtypes. *Nat Rev Nephrol*. 2017;13(8):483–495. doi:10.1038/nrneph.2017.85
6. Chang A, Clark MR, Ko K. Cellular aspects of the pathogenesis of lupus nephritis. *Curr Opin Rheumatol*. 2021;33(2):197–204. doi:10.1097/BOR.0000000000000777
7. Wang S, Wu M, Chiriboga L, et al. Membrane attack complex (MAC) deposition in renal tubules is associated with interstitial fibrosis and tubular atrophy: a pilot study. *Lupus Sci Med*. 2022;9(1):e000576. doi:10.1136/lupus-2021-000576
8. Yu F, Wu LH, Tan Y, et al. Tubulointerstitial lesions of patients with lupus nephritis classified by the 2003 international society of nephrology and renal pathology society system. *Kidney Int*. 2010;77(9):820–829. doi:10.1038/ki.2010.13
9. Gomes MF, Mardones C, Xipell M, et al. The extent of tubulointerstitial inflammation is an independent predictor of renal survival in lupus nephritis. *J Nephrol*. 2021;34(6):1897–1905. doi:10.1007/s40620-021-01007-z
10. Wilson PC, Kashgarian M, Moeckel G. Interstitial inflammation and interstitial fibrosis and tubular atrophy predict renal survival in lupus nephritis. *Clin Kidney J*. 2018;11(2):207–218. doi:10.1093/ckj/sfx093
11. Abraham R, Durkee MS, Ai J, et al. Specific in situ inflammatory states associate with progression to renal failure in lupus nephritis. *J Clin Invest*. 2022;132(13):e155350. doi:10.1172/JCI155350
12. Hong S, Healy H, Kassianos AJ. The emerging role of renal tubular epithelial cells in the immunological pathophysiology of lupus nephritis. *Front Immunol*. 2020;11:578952. doi:10.3389/fimmu.2020.578952
13. Newman AM, Liu CL, Green MR, et al. Robust enumeration of cell subsets from tissue expression profiles. *Nat Methods*. 2015;12(5):453–457. doi:10.1038/nmeth.3337
14. Murea M, Park JK, Sharma S, et al. Expression of Notch pathway proteins correlates with albuminuria, glomerulosclerosis, and renal function. *Kidney Int*. 2010;78(5):514–522. doi:10.1038/ki.2010.172
15. Li Y, Yuan Y, Huang ZX, et al. GSDME-mediated pyroptosis promotes inflammation and fibrosis in obstructive nephropathy. *Cell Death Differ*. 2021;28(8):2333–2350. doi:10.1038/s41418-021-00755-6
16. Papa V, Brainer J, Henriksen KJ, et al. Extraglomerular immune complex deposition in lupus nephritis. *Lupus*. 2022;31(1):19–27. doi:10.1177/09612033211062535
17. Hsieh C, Chang A, Brandt D, et al. Predicting outcomes of lupus nephritis with tubulointerstitial inflammation and scarring. *Arthritis Care Res*. 2011;63(6):865–874. doi:10.1002/acr.20441
18. Pagni F, Galimberti S, Galbiati E, et al. Tubulointerstitial lesions in lupus nephritis: international multicentre study in a large cohort of patients with repeat biopsy. *Nephrology*. 2016;21(1):35–45. doi:10.1111/nep.12555
19. Espeli M, Bökers S, Giannico G, et al. Local renal autoantibody production in lupus nephritis. *J Am Soc Nephrol*. 2011;22(2):296–305. doi:10.1681/ASN.2010050515
20. Chen J, Cui L, Ouyang J, et al. Clinicopathological significance of tubulointerstitial CD68 macrophages in proliferative lupus nephritis. *Clin Rheumatol*. 2022;41(9):2729–2736. doi:10.1007/s10067-022-06214-y
21. Suárez-Fueyo A, Rojas JM, Cariaga AE, et al. Inhibition of PI3Kδ reduces kidney infiltration by macrophages and ameliorates systemic lupus in the mouse. *J Immunol*. 2014;193(2):544–554. doi:10.4049/jimmunol.1400350
22. Sandersfeld M, Büttner-Herold M, Ferrazzi F, et al. Macrophage subpopulations in pediatric patients with lupus nephritis and other inflammatory diseases affecting the kidney. *Arthritis Res Ther*. 2024;26(1):46. doi:10.1186/s13075-024-03281-1

23. Cao Q, Harris DC, Wang Y. Macrophages in kidney injury, inflammation, and fibrosis. *Physiology*. 2015;30(3):183–194. doi:10.1152/physiol.00046.2014
24. Nikolic-Paterson DJ, Wang S, Lan HY. Macrophages promote renal fibrosis through direct and indirect mechanisms. *Kidney Int Suppl*. 2014;4(1):34–38. doi:10.1038/kisup.2014.7
25. Huen SC, Cantley LG. Macrophages in renal injury and repair. *Annu Rev Physiol*. 2017;79(1):449–469. doi:10.1146/annurev-physiol-022516-034219
26. Wang X, Fu S, Yu J, et al. Renal interferon-inducible protein 16 expression is associated with disease activity and prognosis in lupus nephritis. *Arthritis Res Ther*. 2023;25(1):112. doi:10.1186/s13075-023-03094-8
27. Liao JC, Lam R, Brazda V, et al. Interferon-inducible protein 16: insight into the interaction with tumor suppressor p53. *Structure*. 2011;19(3):418–429. doi:10.1016/j.str.2010.12.015
28. Kim H, Kim H, Feng Y, et al. PRMT5 control of cGAS/STING and NLRC5 pathways defines melanoma response to antitumor immunity. *Sci Transl Med*. 2020;12(551):eaaz5683. doi:10.1126/scitranslmed.aaz5683
29. Baggetta R, De Andrea M, Gariano GR, et al. The interferon-inducible gene IFI16 secretome of endothelial cells drives the early steps of the inflammatory response. *Eur J Immunol*. 2010;40(8):2182–2189. doi:10.1002/eji.200939995
30. Fan Z, Chen R, Yin W, et al. Effects of AIM2 and IFI16 on infectious diseases and inflammation. *Viral Immunol*. 2023;36(7):438–448. doi:10.1089/vim.2023.0044
31. Zhao H, Gonzalezgugel E, Cheng L, et al. The roles of interferon-inducible p200 family members IFI16 and p204 in innate immune responses, cell differentiation and proliferation. *Genes Dis*. 2015;2(1):46–56. doi:10.1016/j.gendis.2014.10.003
32. Gugliesi F, De Andrea M, Mondini M, et al. The proapoptotic activity of the Interferon-inducible gene IFI16 provides new insights into its etiopathogenetic role in autoimmunity. *J Autoimmun*. 2010;35(2):114–123. doi:10.1016/j.jaut.2010.04.001
33. Fu Q, He Q, Dong Q, et al. The role of cyclic GMP-AMP synthase and Interferon-I-inducible protein 16 as candidatebiomarkers of systemic lupus erythematosus. *Clin Chim Acta*. 2022;524:69–77. doi:10.1016/j.cca.2021.11.003
34. Chen JX, Cheng CS, Gao HF, et al. Overexpression of interferon-inducible protein 16 promotes progression of human pancreatic adenocarcinoma through interleukin-1β-induced tumor-associated macrophage infiltration in the tumor microenvironment. *Front Cell Dev Biol*. 2021;9:640786. doi:10.3389/fcell.2021.640786
35. Wang B, Guo H, Yu H, Chen Y, Xu H, Zhao G. The role of the transcription factor EGR1 in cancer. *Front Oncol*. 2021;11:642547. doi:10.3389/fonc.2021.642547
36. Zou K, Zeng Z. Role of early growth response 1 in inflammation-associated lung diseases. *Am J Physiol Lung Cell Mol Physiol*. 2023;325(2):L143–L154. doi:10.1152/ajplung.00413.2022
37. Ho LC, Sung JM, Shen YT, et al. Egr-1 deficiency protects from renal inflammation and fibrosis. *J Mol Med*. 2016;94(8):933–942. doi:10.1007/s00109-016-1403-6
38. Okabe M, Koike K, Yamamoto I, Tsuboi N, Matsusaka T, Yokoo T. Early growth response 1 as a podocyte injury marker in human glomerular diseases. *Clin Kidney J*. 2023;17(1):sfad289. doi:10.1093/ckj/sfad289
39. Haller O, Kochs G. Mx genes: host determinants controlling influenza virus infection and trans-species transmission. *Hum Genet*. 2020;139(6–7):695–705. doi:10.1007/s00439-019-02092-8
40. Haller O, Staeheli P, Schwemmle M, Kochs G. Mx GTPases: dynamin-like antiviral machines of innate immunity. *Trends Microbiol*. 2015;23(3):154–163. doi:10.1016/j.tim.2014.12.003
41. Joseph S, George NI, Green-Knox B, et al. Epigenome-wide association study of peripheral blood mononuclear cells in systemic lupus erythematosus: identifying DNA methylation signatures associated with interferon-related genes based on ethnicity and SLEDAI. *J Autoimmun*. 2019;96:147–157. doi:10.1016/j.jaut.2018.09.007
42. Cecchi I, Radin M, Barinotti A, et al. Type I interferon pathway activation across the antiphospholipid syndrome spectrum: associations with disease subsets and systemic antiphospholipid syndrome presentation. *Front Immunol*. 2024;15:1351446. doi:10.3389/fimmu.2024.1351446
43. Raupov RK, Suspitsin EN, Kalashnikova EM, et al. IFN-I score and rare genetic variants in children with systemic lupus erythematosus. *Biomedicines*. 2024;12(6):1244. doi:10.3390/biomedicines12061244
44. Juárez-Vicuña Y, Pérez-Ramos J, Adalid-Peralta L, et al. Interferon Lambda 3/4 (IFNλ3/4) rs12979860 polymorphisms is not associated with susceptibility to systemic lupus erythematosus, although it regulates OASL expression in patients with SLE. *Front Genet*. 2021;12:647487. doi:10.3389/fgene.2021.647487
45. Shimizu Y, Yasuda S, Kimura T, et al. Interferon-inducible Mx1 protein is highly expressed in renal tissues from treatment-naïve lupus nephritis, but not in those under immunosuppressive treatment. *Mod Rheumatol*. 2018;28(4):661–669. doi:10.1080/14397595.2017.1404711